

Multiple polarization orange and red laser emissions with Pr:BaY₂F₈

Alberto Sottile,^{1,*} Daniela Parisi,^{1,2} and Mauro Tonelli^{1,2}

¹Dipartimento di Fisica, Università di Pisa, Largo B. Pontecorvo 3, Pisa, 56127, Italy

²NEST, Istituto di Nanoscienze – CNR, Piazza S. Silvestro, 12, Pisa, 56127, Italy

*sottile@df.unipi.it

Abstract: We investigated the polarization of continuous-wave laser emission in the orange region, at 607 nm, and in the red region, at 639 nm and 643 nm, from a Pr:BaY₂F₈ (Pr:BYF) crystal, pumped by a 445 nm laser diode. We achieved linearly polarized emission along two optic axes of the crystal by changing its orientation with respect to the pump. Simultaneous emission of two orthogonal linear polarizations was observed in the orange region, at the same wavelength, and in the red region, with concurrent emission from the two separate lines.

©2014 Optical Society of America

OCIS codes: (140.3480) Lasers, diode-pumped; (140.3580) Lasers, solid-state; (140.7300) Visible lasers; (160.5690) Rare earth doped materials; (300.6280) Spectroscopy, fluorescence and luminescence.

References and links

1. R. G. Smart, J. N. Carter, A. C. Tropper, D. C. Hanna, S. T. Davey, S. F. Carter, and D. Szebesta, "CW room temperature operation of praseodymium-doped fluorozirconate glass fibre lasers in the blue-green, green and red spectral regions," *Opt. Commun.* **86**(3-4), 333–340 (1991).
2. D. Pabœuf, O. Mhibik, F. Bretenaker, P. Goldner, D. Parisi, and M. Tonelli, "Diode-pumped Pr:BaY₂F₈ continuous-wave orange laser," *Opt. Lett.* **36**(2), 280–282 (2011).
3. M. Fibrich, H. Jelínková, J. Šulc, K. Nejezchleb, and V. Škoda, "Visible cw laser emission of GaN-diode pumped Pr:YAlO₃ crystal," *Appl. Phys. B* **97**(2), 363–367 (2009).
4. A. Richter, N. Pavel, E. Heumann, G. Huber, D. Parisi, A. Toncelli, M. Tonelli, A. Diening, and W. Seelert, "Continuous-wave ultraviolet generation at 320 nm by intracavity frequency doubling of red-emitting Praseodymium lasers," *Opt. Express* **14**(8), 3282–3287 (2006).
5. T. Sandrock, T. Danger, E. Heumann, G. Huber, and B. H. T. Chai, "Efficient Continuous Wave-laser emission of Pr³⁺-doped fluorides at room temperature," *Appl. Phys. B* **58**(2), 149–151 (1994).
6. A. Richter, E. Heumann, E. Osiac, G. Huber, W. Seelert, and A. Diening, "Diode pumping of a continuous-wave Pr³⁺-doped LiYF₄ laser," *Opt. Lett.* **29**(22), 2638–2640 (2004).
7. F. Cornacchia, A. Richter, E. Heumann, G. Huber, D. Parisi, and M. Tonelli, "Visible laser emission of solid state pumped LiLuF₄:Pr³⁺," *Opt. Express* **15**(3), 992–1002 (2007).
8. S. Khiari, M. Velazquez, R. Moncorgé, J. L. Doualan, P. Camy, A. Ferrier, and M. Diaf, "Red-luminescence analysis of Pr³⁺-doped fluoride crystals," *J. Alloy. Comp.* **451**(1-2), 128–131 (2008).
9. L. H. Guilbert, J. Y. Gesland, A. Bulou, and R. Retoux, "Structure and Raman spectroscopy of Czochralski-grown barium yttrium and barium ytterbium fluorides crystals," *Mater. Res. Bull.* **28**(9), 923–930 (1993).
10. A. Toncelli, M. Tonelli, A. Cassanho, and H. P. Jenssen, "Spectroscopy and dynamic measurements of a Tm,Dy:BaY₂F₈ crystal," *J. Lumin.* **82**(4), 291–298 (1999).
11. R. McFarlane, "Upconversion laser in BaY₂F₈:Er 5% pumped by ground-state and excited-state absorption," *J. Opt. Soc. Am. B* **11**(5), 871–880 (1994).
12. F. Cornacchia, D. Parisi, C. Bernardini, A. Toncelli, and M. Tonelli, "Efficient, diode-pumped Tm³⁺:BaY₂F₈ vibronic laser," *Opt. Express* **12**(9), 1982–1989 (2004).
13. André Richter, *Laser Parameters and Performance of Pr³⁺-doped Fluorides Operating in the Visible Spectral Region* (Cuvillier Verlag, 2008).
14. M. Scheller, J. M. Yarborough, J. V. Moloney, M. Fallahi, M. Koch, and S. W. Koch, "Room temperature continuous wave milliwatt terahertz source," *Opt. Express* **18**(26), 27112–27117 (2010).

1. Introduction

Praseodymium (Pr) trivalent ions have been intensively studied due to their transitions in the visible range, which have been exploited in several solid-state lasers. Laser emission with Pr-doped materials have been demonstrated in green, orange, red and near-infrared regions [1–3]. The orange transition is particularly interesting due to the lack of sources in the same

wavelength range, while the red transition have been investigated as input source for second harmonic generation devices, in order to obtain laser emission in the UV range [4].

These levels of Pr have been investigated in various host materials, but over the years fluoride crystals have shown the best optical qualities and laser performances [5]. Extensive research has been conducted with uniaxial fluoride crystals, such as LiYF_4 and LiLuF_4 [6,7]. However, fewer studies have been carried out on monoclinic crystals, such as BaY_2F_8 (Barium Yttrium Fluoride or BYF), which have three different crystallographic axes. This reduced symmetry splits further the Pr levels inside the host, causing the appearance of new emission lines [8].

We report a spectroscopic characterization of a Pr-doped BYF crystal along all its optic axes for the orange and red regions. From these measurements we observed three emission lines: 607 nm, 639 nm and 643 nm. We obtained continuous-wave laser emission linearly polarized along two optic axes, in the orange region, at 607 nm, and in the red region, from both the lines. Simultaneous emission with two orthogonal polarizations was observed at 607 nm. In addition to that, we achieved concurrent laser emission from the two red lines.

To the best of our knowledge, this is the first investigation of the polarization of laser emissions in this material, as a function of the orientation of the crystal, in this range of wavelengths. As far as we know, this work is also the first report of laser emission at 643 nm from Pr:BYF.

2. Experimental

We studied a sample of monocrystalline BYF, doped with Pr ions at 1.25% at. concentration in the melt. BYF has a monoclinic structure, with unit cell parameters $a = 6.983 \text{ \AA}$, $b = 10.519 \text{ \AA}$ and $c = 4.264 \text{ \AA}$. The angle between the a -axis and the c -axis, called β , is 99.68° . The symmetry group of BYF lattice is C_2/m and the unit cell contains two molecules. This host had been proven to be transparent from the UV to the IR region ($0.2\text{-}9 \mu\text{m}$), with a refractive index of 1.5 [9,10].

During the optical characterization we refer to the optic axes (x,y,z) of the lattice, instead of the crystallographic ones. In BYF, the y -axis is coincident with b , while x and z are in the plane that contains a and c . There is an angle of about 11° between the x and a axes [11].

2.1 Crystal growth and cut

Crystal growth was performed in a homemade Czochralski furnace, located in our laboratories, designed to ensure high optical quality of the resulting samples. The main chamber is equipped with conventional resistive heating. This environment is vacuumed to a pressure limit of 10^{-7} mbar to remove all the contaminants, then Argon gas is inserted to create an overpressure in the container. The furnace has also an optical feedback system to control diameter of the growing crystal. A full description of the furnace and of the growth procedure is given in [12].

We used BaY_2F_8 powders as starting material, adding the necessary amount of BaF_2 and PrF_3 powders to achieve 1.25% doping concentration in the melt. Pr ions replace Yttrium in the doped crystal. There is a mismatch between the ionic radii of Pr and Yttrium, which leads to a non-uniform doping level inside the whole growth. Previous studies have shown that the concentration of Pr in the crystal varies from 0.4 to 0.5 times the concentration in the melt [13]. The finished product was tested with an X-ray Laue diffractometer to check if it had a single lattice and to identify the crystallographic axes in it. Samples for spectroscopy and laser experiments were cut in a parallelepiped shape, with the optic axes along the edges.

The crystal used in laser experiments was 4.8 mm long in the x -axis, 2.7 mm tall in the y -axis and 3.9 mm wide in the z -axis. All the six facets were polished to reduce roughness and to enhance reflectivity and overall optical quality of the sample. No coating was applied on the facets of the crystal.

2.2 Spectroscopy

Absorption spectra were measured with a Varian CARY 500 spectrophotometer, between 430 nm and 490 nm, with a resolution of 0.15 nm, to identify suitable wavelengths for pumping the crystal and achieve laser emission.

Fluorescence from the sample was acquired while pumping it with a 445 nm laser diode at 80 mW. Light emitted by the crystal was chopped, filtered to remove spurious scattering from the pump, focused on a monochromator with a 1200 g/mm diffraction grating and then sampled with a R1464 Hamamatsu photomultiplier. This signal was sent to a lock-in amplifier and acquired from a PC. We placed a Glan-Thompson polarizer at the input slit of the monochromator to collect the components of the emission one at a time. The acquired spectra were corrected for the optical response of the system using a blackbody source at 3000 K.

Fluorescence was measured for light polarized along the three optic axes of the crystal, at wavelengths between 465 nm and 750 nm, with a resolution of 0.13 nm.

2.3 Laser cavity

We designed the laser experiment to measure the continuous-wave performances of the crystal with respect to its orientation. The sample was placed in a nearly hemispherical resonant cavity. We employed a continuous-wave 445 nm InGaN laser diode at 1.5 W as pump source, focused on the cavity with a 30 mm achromatic lens. Emission of the pump laser was linearly polarized. The pump beam had a rectangular shape with the dimensions of 2.4 mm by 1.5 mm. The input power sent to the cavity was tuned using a continuously variable neutral density placed ahead of the focusing lens.

The input coupler (IC) plane mirror had a face with anti-reflection (AR) coating between 420 nm and 520 nm ($T > 99\%$) and the other with a high reflectivity (HR) coating between 590 nm and 700 nm ($R > 99\%$). We used alternatively two hemispherical mirrors as output couplers (OC), with different coating on the round face. One of them was HR coated between 620 nm and 640 nm ($T = 5\%$), with a broad tail that extended also in the orange region. Transmittance of this mirror at 607 nm was about 5.5%. The other OC mirror was HR coated in a narrow bandwidth going from 630 nm to 650 nm ($T = 0.5\%$), hence suitable for the red region. Both the OC mirrors had a radius of curvature of 50 mm.

We placed the crystal in a copper holder with water at 18 °C circulating inside, employed to cool it down during the measurements. This holder was fixed on a goniometric head capable of rotating and translating the sample along the two horizontal directions. In addition to that, a horizontal translation stage was employed to sustain the OC mirror and optimize the cavity length, which was kept near 5 cm.

Light coming from the OC was filtered with a 510 nm long pass filter to remove the fraction of input laser passing through the cavity. Output power was measured with a Silicon power meter. The wavelength of the emission was measured using an Ocean Optics HR4000 portable spectrophotometer, with a resolution of 1 nm. Polarization of the output laser was determined with an adjustable Glan-Thompson polarizer placed in front of the OC mirror, outside the cavity.

3. Spectroscopic characterization

3.1 Absorption spectra

Results of the absorption measurements performed on the crystal are shown in Fig. 1. All the polarizations are reported. Absorption from the ground level to the 3P_2 sublevel is visible at about 445 nm. Data show that the sample can be pumped at those wavelengths, with a maximum absorption coefficient of 4.0 cm^{-1} for light polarized parallel to the y -axis.

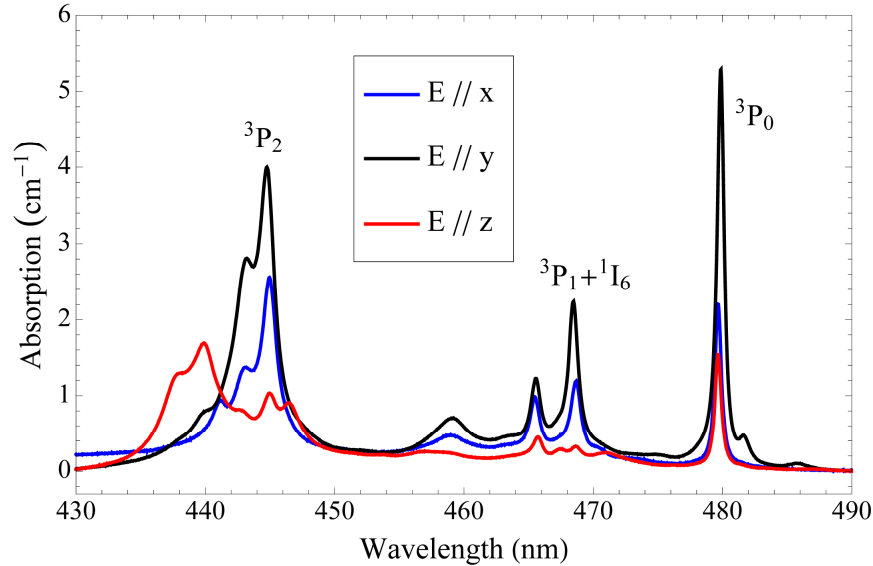


Fig. 1. Room temperature polarized absorption spectra of Pr:BYF.

3.2 Fluorescence spectra

Figure 2 shows the emission spectra of the sample, for all the polarizations, between 600 nm and 650 nm. Two transitions have been identified and labeled in the plot. The interaction with the crystal lattice cause several peaks in the fluorescence emitted from a single transition. In particular, the red manifold divides into two peaks, at 639 nm and 643 nm. The relative heights of those peaks are also altered; for example, for light parallel polarized along the z -axis, the fluorescence is more intense at 639 nm than at 643 nm, while the opposite behavior happens for $E // y$. This effect can be exploited to maximize the emission of one of the two lines and suppress the other.

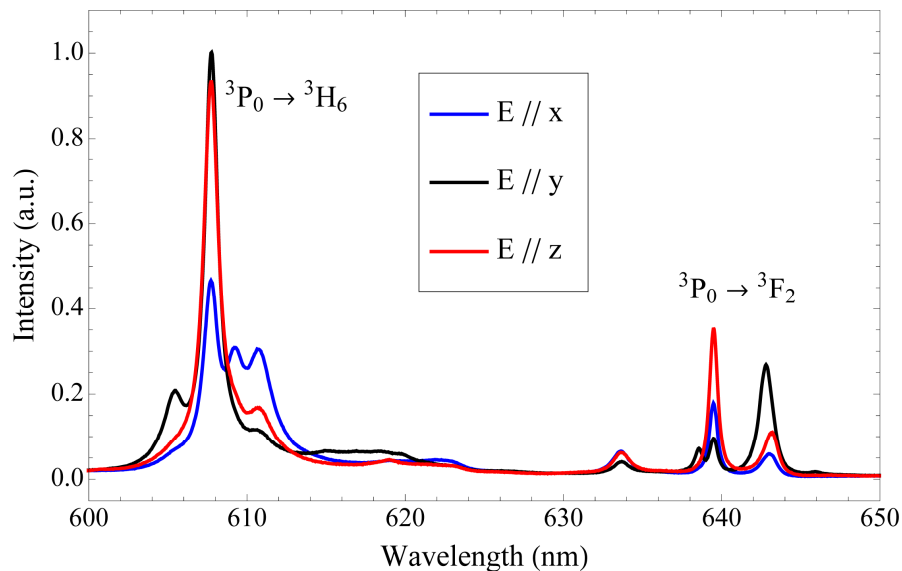


Fig. 2. Room temperature polarized emission spectra of Pr:BYF.

Figure 2 also allows to determine which polarization has the highest gain for all the emission lines. For example, the orange line is preferably emitted parallel to the y -axis.

4. Laser experiments

The sample prepared for laser measurements was placed in the cavity in three different positions, with the pump laser directed at the x - y facet, at the x - z facet or at the y - z facet. Polarization of the pump was aligned to the axis with the higher absorption, for example y in the x - y facet or z in the x - z facet. Emission wavelength range was selected by choosing the OC mirror with the right coating. Thus, we employed the 5% OC mirror to achieve laser emission in the orange region, or the 0.5% OC mirror for the red transitions.

4.1 x - y orientation

In the orange region, using the 5% OC mirror, we achieved laser emission at 607 nm, polarized along the y -axis of the crystal. The maximum output power was 64 mW.

In the red region, with the 0.5 OC mirror, the crystal emitted at 643 nm with light polarized along its y -axis. A plot of the output power at this wavelength, as a function of the power absorbed from the sample is shown in Fig. 3. We report slope efficiency with respect to power absorbed from the crystal (η_{abs}) and threshold absorbed power of laser emission (W_{thr}). The orientation of the crystal is also depicted in the same figure. The maximum output power was 17 mW, with 2.6% slope efficiency. In this orientation, emission from the 639 nm line was suppressed because the z -axis was aligned with the pump beam, hence it could not emit.

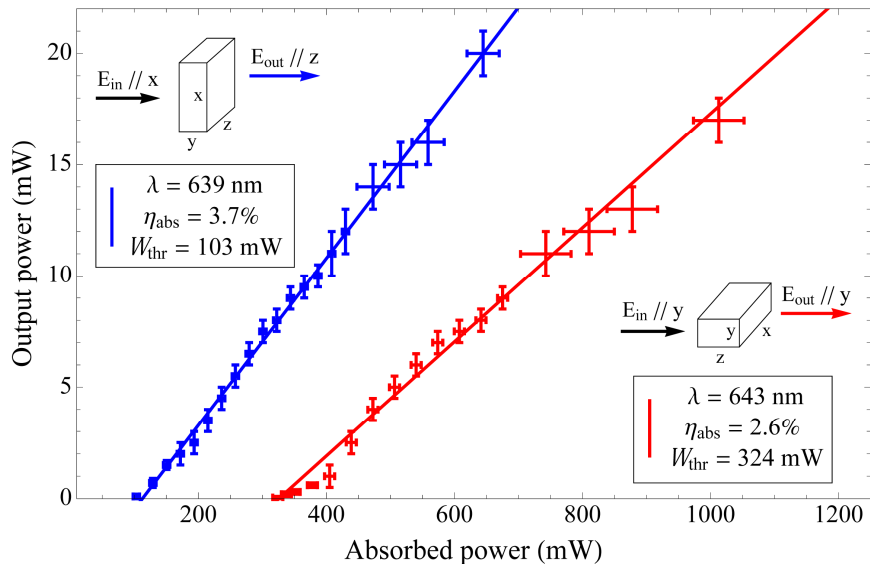


Fig. 3. Output powers for the red region, as functions of absorbed power, at 639 nm and at 643 nm. Slope efficiencies (η_{abs}) and threshold powers (W_{thr}) are also indicated.

4.2 x - z orientation

In the orange region, with the 5% OC mirror, the sample exhibited laser emission at 607 nm, with polarization parallel to its z -axis. In this case, emission from the y -axis was inhibited and fluorescence coming from the x -axis was much less intense than the one from the z -axis. We obtained a maximum output power of 30 mW.

In the red region, using the 0.5% OC mirror, laser emission was observed at 639 nm, with polarization along the z -axis of the crystal. Figure 3 shows the output powers and the alignment of the crystal for this emission. Unlike the previous case, in this orientation the line at 643 nm was suppressed because the y -axis was parallel to the pump beam.

4.3 *y*-*z* orientation

With the crystal in this orientation, we observed changes in the polarization of the emission by tuning the cavity length around the highest output power. Alterations in the cavity layout introduce losses in one polarization or in the other. By exploiting this effect, we observed steady laser emission, in both orange and red regions, completely parallel polarized along the *y*-axis, completely polarized along the *z*-axis, or simultaneously polarized along both *y*- and *z*-axes. Optimizing the output power to reach the maximum constrained the crystal to emit only the polarization with the highest fluorescence intensity.

In the orange region, using the 5% OC mirror, we observed emission at 607 nm with $E // y$ and with $E // z$. The maximum power was reached for the emission parallel polarized along the *y*-axis. We characterized output power of this emission as a function of absorbed power. Data obtained from these measurements are depicted in Fig. 4. A scheme of the orientation of the sample is also shown in the same figure. We also obtained emission simultaneously polarized along both *y*- and *z*- axes. In the most stable conditions, we measured an output power of 85 mW, formed by 45 mW, with $E // y$; and by 40 mW, with $E // z$, with the same wavelength.

We checked the beam quality of the simultaneous orange emission using a Coherent ModeMaster MMH-2S beam propagation analyzer. The M^2 parameter of the emission was 3.2 along the *y*-axis and 1.9 along the *z*-axis of the crystal. We also measured the laser beam waist, obtaining 220 μm for $E // y$ and 90 μm for $E // z$.

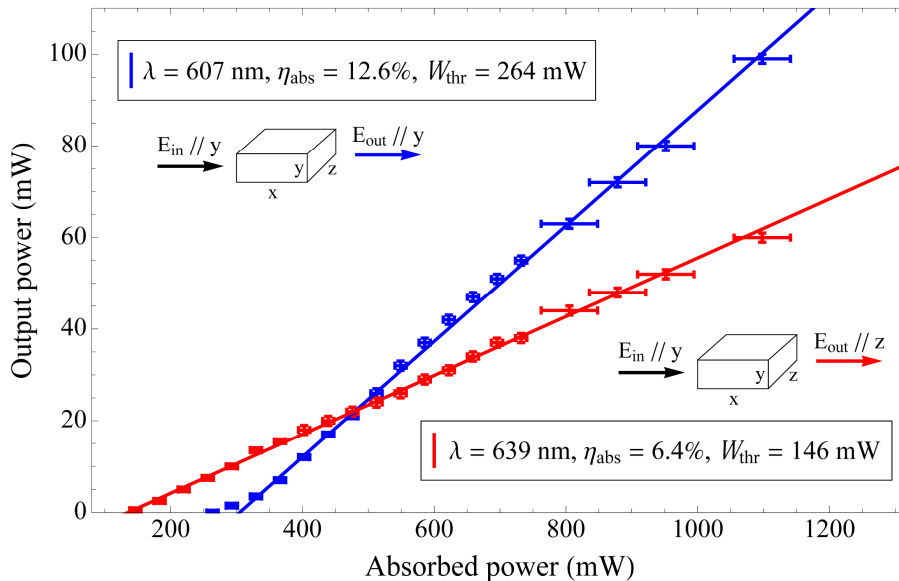


Fig. 4. Output power as a function of absorbed power at 607 nm and 639 nm with the sample in *y*-*z* orientation. Slope efficiencies (η_{abs}) and threshold powers (W_{thr}) are also indicated.

In the red region, with this crystal orientation, we observed a peculiar effect. By changing the length of the cavity we obtained laser emission in three different stable modes: emission at 639 nm, polarized along the *z*-axis; emission at 643 nm, polarized along the *y*-axis; and simultaneous emission at the two wavelengths, each one with its polarization. Resonant modes inside the cavity are shifted by length alterations, leading to enhancement of one of the two wavelengths and depletion of the other. There are also length values that allow resonance of both wavelengths at the same time.

Optimizing the output power forced the system to emit at 639 nm, with $E // z$. We measured the maximum output power in this condition as a function of the absorbed power. Results of this experiment are reported in Fig. 4.

During concurrent emission, in the most stable conditions, we achieved a total output power of 48 mW, divided in 26 mW at 639 nm, along the z -axis; and in 22 mW at 643 nm, parallel to the y -axis of the crystal. A spectrum of the output laser acquired during simultaneous emission is shown in Fig. 5, in which the two distinct peaks are clearly visible.

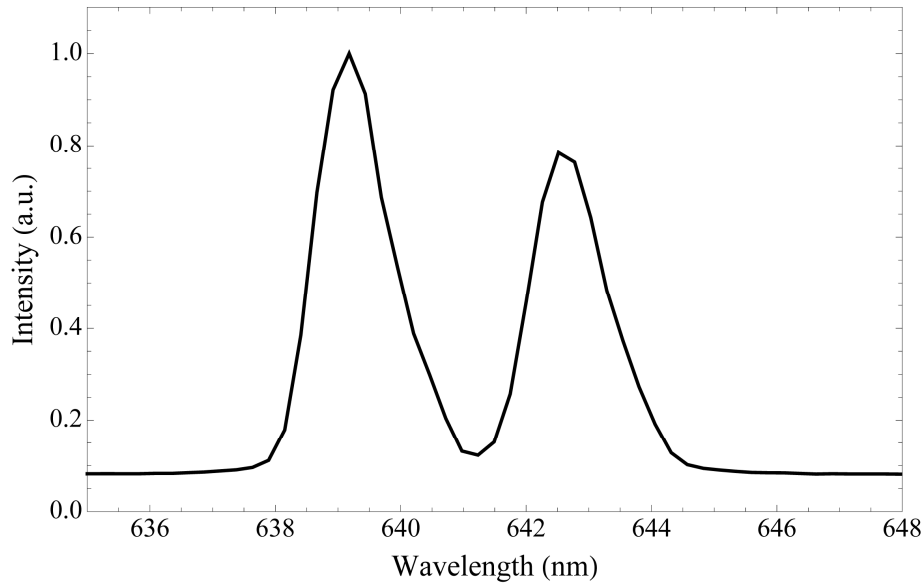


Fig. 5. Spectrum of the simultaneous emission at 639 nm and at 643 nm.

All the single emissions achieved, with respective orientation of the crystal, fraction of absorbed pump power, OC mirror transmittance, output wavelength, output polarization and maximum output power are summarized in Table 1.

Table 1. List of the Observed Single Emissions

	Abs. power	T	λ	E_{out}	W_{max}
x - y orientation $E_{\text{in}} // y$	79%	5%	607 nm	y -axis	64 mW
		0.5%	643 nm	y -axis	17 mW
x - z orientation $E_{\text{in}} // x$	50%	5%	607 nm	z -axis	30 mW
		0.5%	639 nm	z -axis	20 mW
y - z orientation $E_{\text{in}} // y$	86%	5%	607 nm	y -axis	99 mW
		0.5%	639 nm	z -axis	60 mW
		0.5%	643 nm	y -axis	45 mW

The powers obtained during simultaneous emission of two orthogonal polarizations are reported in Table 2.

Table 2. List of the Observed Simultaneous Emissions

	T	λ	E_{out}	W_{max}
<i>y-z</i> orientation	5%	607 nm	<i>y</i> -axis	45 mW
			<i>z</i> -axis	40 mW
$E_{in} // y$	0.5%	639 nm	<i>z</i> -axis	26 mW
			<i>y</i> -axis	22 mW

5. Conclusions and perspectives

We describe the growth and the spectroscopic characterization of a Pr:BYF crystal doped at 1.25%. We measured absorption in the blue region and fluorescence in the orange and red regions. A split of the red transition in two near lines was observed from the fluorescence spectra. We achieved continuous-wave laser emission at 607 nm, at 639 nm and at 643 nm, linearly polarized along different optic axes of the crystal. To the best of our knowledge, this is the first characterization of the orange and red laser emissions from this material with respect to their polarization. This work is also the first report of laser emission at 643 nm from this crystal.

Simultaneous emission of two orthogonal polarizations was also obtained in both regions with a specific orientation of the sample. In the orange region, the wavelength of the two emissions was the same. In the red region, concurrent emission at two different wavelengths was observed. This output could be exploited for difference frequency generation, resulting in an emission in the terahertz range [14].

Acknowledgments

The authors would like to acknowledge I. Grassini for her assistance during the preparation of the samples.